

Deep Learning-powered Iterative Combinatorial Auctions

Jakob Weisstener
University of Zurich
weisstener@ifi.uzh.ch

Stefania Ionescu
University of Zurich
ionescu@ifi.uzh.ch

Nils Olberg
University of Zurich
olberg@ifi.uzh.ch

Sven Seuken
University of Zurich
seuken@ifi.uzh.ch

March 28, 2022

Abstract

In this paper, we study the design of deep learning-powered iterative combinatorial auctions (ICAs). We build on the work by [Brero et al. \(2018\)](#), who have successfully integrated support vector regression (SVR) into the preference elicitation algorithm of an ICA. However, their SVR-based approach also has its limitations because the algorithm requires solving the auction’s winner determination problem (WDP) given predicted value functions. With expressive kernels (like gaussian, exponential or high degree polynomial kernels), the WDP cannot be solved for large domains. While linear or low-degree polynomial kernels have better computational scalability, these kernels have limited expressiveness. In this work, we address these shortcomings by using deep neural networks (DNNs) instead of SVRs for learning bidders’ valuation functions. Our main contribution is to show that the resulting maximization step of DNNs consisting of rectified linear units as activation functions can always be reformulated into a mixed integer linear program (MILP). Preliminary simulation results indicate that even two-hidden-layer-fully-connected DNNs with a small number of hidden units lead to higher economic efficiency than kernelized SVRs with a comparable or even smaller runtime.

Keywords: Combinatorial Auctions, Deep Learning, Mixed Integer Linear Program, Preference Elicitation

1 Introduction

Combinatorial auctions (CAs) are used to allocate several items to bidders who may view these items as complements or substitutes. Specifically, bidders are allowed to submit bids on bundles of items rather than on single items to express their complex preferences. CAs have found widespread real-world applications in billion-dollar domains, including for the sale of spectrum licenses.

One of the main challenges when conducting large CAs in practice is that the bundle space grows exponentially in the number of items, which typically makes it impossible for the bidders to report their full value function, even for medium-sized problems. Thus, it is still a challenging task to elicit the preferences of bidders to obtain a highly efficient allocation as well as to generate a substantial amount of revenue.

Researchers have addressed the preference elicitation problem by designing bidding languages that should, on the one hand, be expressive enough such that a large class of bidders’ valuation functions can be described, and, on the other hand, succinct enough, so that this can be achieved with a small representation size. Unfortunately, it has been shown that in order to guarantee full efficiency and support general valuation functions, exponential communication in the number of items is needed ([Nisan and Segal, 2006](#)). To overcome this issue many recent proposals have focused on *iterative combinatorial auctions (ICAs)*. In ICAs, the goal is typically to find an (approximately) efficient allocation (i) without revealing all 2^m bundles, thus overcoming the curse of dimensionality

and (ii) without placing a burden on bidders to report their valuations in a specific bidding language selected by the auctioneer.

Recently, [Brero et al. \(2018\)](#) proposed a *machine learning-powered ICA*, which achieves higher efficiency than the popular combinatorial clock auction (CCA) in multiple spectrum auction settings. The core of their auction mechanism is a *machine learning-powered preference elicitation algorithm*, which uses value queries to interact with bidders during the auction phase. As part of this preference elicitation method, they used the machine learning algorithm to learn bidders’ valuation functions. For estimating these, they used kernelized support vector regressions (SVRs) as the machine learning algorithm. Kernelized SVRs are a popular non-linear regression technique, where a linear model is fitted on transformed data. The data points are, in our case, the bundle–value pairs in the CA setting. In SVRs, the transformation of bundles is implicitly conducted by setting a suitable kernel function in the definition of the SVRs (see, e.g., [Smola and Schölkopf \(2004\)](#)).

In spite of their success, [Brero et al. \(2018\)](#) faced the following issue in their work: because of the runtime complexity of the resulting maximization step, i.e., the winner determination problem, they focused on linear and quadratic kernels in the implementation of the SVRs for large auction settings. This leaves room for improvement in the estimation step, since bidders’ valuations in spectrum auctions could potentially have more complex structures than could be captured by linear or quadratic kernels. Linear kernels can only model additive preferences, which might be unreasonable to assume in CAs. Although quadratic kernels are more expressive than linear ones, using them in the definition of SVRs results in linear functions on transformed bundles, such that additionally to the original items they take all two-way interactions between items into account. [Brero et al. \(2018\)](#) also experimented with more expressive kernels (gaussian and exponential) but for these kernels, the resulting winner determination problem cannot be solved for large auction settings.

In this paper, we propose to use deep neural networks (DNNs) instead of SVRs in machine learning-powered CAs, and we study how this can be achieved and what (if any) efficiency improvements can be obtained. DNNs do not use predefined feature transformations as in the quadratic kernel case but implicitly learn features from bids in the process of training. On a technical level, we show how to reformulate the optimization problem in the preference elicitation algorithm with DNNs consisting of rectified linear units as activation functions into a mixed integer linear program (MILP) (Section 3). This can be achieved by introducing binary variables that model the state (active or non-active) of each node in the DNN. It is noteworthy that the resulting MILP is always linear, independent of the model complexity (number of hidden layers and nodes) of the DNNs. This is in contrast to the WDP for SVRs when non-linear kernels are used (for example, with the quadratic kernel, the WDP becomes a QIP). Furthermore, in contrast to SVRs, the MILP resulting from using DNNs is independent of the number of training points. However, this last property may be less important in the CA setting, since usually only a small number of initial bids, on which the learning algorithms are trained on, is considered. Recently, [Fischetti and Jo \(2017\)](#) proposed a similar approach of optimizing fitted DNNs via a reformulation into a MILP for the problem of finding adversarial examples in image recognition.

To test the performance of our approach, we use the the spectrum auction test suite SATS ([Weiss et al., 2017](#)) to generate synthetic CA instances (Section 4). We conduct several experiments on estimation accuracy and economic efficiency in the Local Synergy Value Model (LSVM). Our results show that even small-sized neural networks are superior to linear, quadratic, gaussian and exponential kernels in (1) terms of capturing bidders’ valuations, (2) the resulting efficiency of the preference elicitation algorithm and (3) the resulting efficiency of the entire auction mechanism. In Section 5, we briefly discuss our ongoing research. We are currently comparing the performance of our DNN-based approach against the SVR-based approach in more and larger spectrum auction domains. To ultimately design an optimal DNN architecture, we will experimentally investigate the trade-off between model complexity and the scalability of the resulting maximization step.

2 Preliminaries

2.1 Setting

In this section, we present the combinatorial auction (CA) setting, following Brero et al. (2018). Let n denote the number of participating bidders and m the number of indivisible items auctioned off in a CA. Furthermore, let $N := \{1, \dots, n\}$ and $M := \{1, \dots, m\}$ be the set of bidders and items, respectively. We denote by $x^i \in \mathcal{X} := \{0, 1\}^m$, $i \in N$ a bundle corresponding to the i^{th} bidder, represented as an indicator vector, where $x_j^i = 1$ if bidder i demands item $j \in M$. By $x := (x^1, \dots, x^n) \in \{0, 1\}^{mn} = \mathcal{X}^n$, we denote an allocation of bundles to bidders¹. Bidders' true preferences over bundles are represented by their true valuation functions $v_i : \{0, 1\}^m \rightarrow \mathbb{R}_+$, $i \in N$, which are assumed to be private knowledge. Consequently, $v_i(x^i)$ represents the true value of the i^{th} bidder for the bundle x^i . Let $v := (v_1, \dots, v_n)$ denote the vector of bidders' valuation functions and $v_{-i} := (v_1, \dots, v_{i-1}, v_{i+1}, \dots, v_n)$ the vector of valuation functions if bidder i is excluded. An allocation x is *feasible* if each item is at most allocated to one bidder, i.e., $\forall j \in M : \sum_{i \in N} x_j^i \leq 1$. We denote the set of feasible allocations by $\mathcal{F} := \{x \in \mathcal{X}^n : \sum_{i \in N} x_j^i \leq 1, \forall j \in M\}$. The payment function is defined as $p(x) = (p_1(x), \dots, p_n(x)) \in \mathbb{R}^n$, with $p_i(x)$ denoting the amount charged to bidder i in allocation x .

Brero et al. (2018) designed an ICA driven by an auction protocol that asks bidders to iteratively report their (possibly untruthful) valuations $\hat{v}_i(\cdot)$ for particular bundles selected by the protocol/algorithm. Based on all reported values until termination, the ICA determines a feasible allocation $x \in \mathcal{F}$ and charges payments $p_i(x)$, $i \in N$. We assume that bidders have quasi-linear utility functions $u_i(x) := v_i(x^i) - p_i(x)$. The *social welfare* of an allocation x is defined as

$$V(x) := \sum_{i \in N} v_i(x^i).$$

Let $x^* \in \arg \max_{x \in \mathcal{F}} V(x)$ be a feasible, social-welfare maximizing, i.e., *efficient*, allocation given the vector of true valuation functions v . Then, the efficiency of any feasible allocation $x \in \mathcal{F}$ is measured in terms of x^* by

$$\frac{V(x)}{V(x^*)}.$$

Furthermore, we let $\hat{\vartheta}_i := \{((x^i)^{(k)}, \hat{v}_i((x^i)^{(k)}))\}_{k \in K_i \subset \mathbb{N}}$ denote a set of reported bundle–value pairs of bidder i , and $\hat{\vartheta} := \bigcup_{i \in N} \hat{\vartheta}_i$ denotes the union of these over all bidders. We define the *reported social welfare* of an allocation x given a set of reported bundle–value pairs $\hat{\vartheta}$ by

$$\hat{V}(x, \hat{\vartheta}) := \sum_{i \in N : (x^i, \hat{v}_i(x^i)) \in \hat{\vartheta}_i} \hat{v}_i(x^i).$$

Finally, the optimal feasible allocation $x_{\hat{\vartheta}}^*$ given reported bundle–value pairs $\hat{\vartheta}$ is defined as

$$x_{\hat{\vartheta}}^* \in \arg \max_{x \in \mathcal{F}} \hat{V}(x, \hat{\vartheta}).$$

The preference elicitation problem in iterative combinatorial auctions using value queries is to find an (approximately) efficient allocation given only a small subset of reported bundle–value pairs

¹Throughout the paper, we will, with slight abuse of notation, denote by x^i a bundle corresponding to the i^{th} bidder in an allocation x as well as a generic element of $\{0, 1\}^m$ (i.e., a "generic bundle"). The meaning should be clear from context.

elicited with value queries. This can be stated more formally as:

Problem 1 (PREFERENCE ELICITATION). *Given a constraint on the number of value queries κ in an ICA, elicit from each bidder a set of reported bundle–value pairs \hat{v} such as to maximize the resulting efficiency, i.e., such as to maximize the following:*

$$\frac{V(x_{\hat{v}}^*)}{V(x^*)}.$$

In most ICAs, a *small* cap on the number of value queries is chosen, e.g., $\kappa \in \{50, \dots, 500\}$.

2.2 Problem Formulation

In this section, we describe the problem formulation of using a machine learning (ML) algorithm – specifically DNNs in our approach – in the preference elicitation algorithm. This problem is different than conducting a plain regression on given bids using an arbitrary ML algorithm, because the arg max of the estimated regression function has to be found in each iteration. This induces an additional challenge. Brero et al. (2018) chose to use SVRs as the ML algorithm, where the optimization step was, at least for linear and quadratic kernels, computationally tractable. In this case, they were able to reformulate the optimization problem to an integer- and quadratic-integer-program, respectively. We will first describe the application of DNNs in the preference elicitation algorithm on a high level. Technical details of the reformulation of the optimization problem into a MILP will be presented later in Section 3.

Recall the *ML-based preference elicitation algorithm* defined in Algorithm 1, which was presented in Brero et al. (2018) in Chapter 2.² This algorithm is a procedure to determine a set of reported bundle–value pairs \hat{v} . It uses an ML algorithm to estimate each bidder’s valuation function. Given these estimated valuation functions, an optimization problem is solved and value queries on bundles that maximize the estimated social welfare function \tilde{V}^t are conducted. In this paper, we focus on Line 4 and Line 5. A detailed line by line description can be found in Brero et al. (2018).

²We slightly changed the notation of a bundle for the i^{th} bidder from a_i^t to $(x^{(t)})^i$ for later convenience.

Algorithm 1: ML-BASED ELICITATION ALGORITHM (Brero et al. (2018))

Parameter : Machine learning algorithm \mathcal{A}

- 1 $\hat{\vartheta}^0$ = initial vector of reported bundle–value pairs, $t = 0$
- 2 **do**
- 3 $t \leftarrow t + 1$
- 4 Estimate social welfare function $\tilde{V}^t := \mathcal{A}(\hat{\vartheta}^{t-1})$
- 5 Determine allocation $x^{(t)} \in \arg \max_{x \in \mathcal{F}} \tilde{V}^t(x; \hat{\vartheta}^{t-1})$
- 6 **for** each bidder i **do**
- 7 **if** $(x^{(t)})^i \notin \hat{\vartheta}_i^{t-1}$ **then**
- 8 Query value $\hat{v}_i((x^{(t)})^i)$
- 9 $\hat{\vartheta}_i^t = \hat{\vartheta}_i^{t-1} \cup ((x^{(t)})^i, \hat{v}_i((x^{(t)})^i))$
- 10 **else**
- 11 $\hat{\vartheta}_i^t = \hat{\vartheta}_i^{t-1}$
- 12 **end**
- 13 **end**
- 14 **while** $\exists i \in N : (x^{(t)})^i \notin \hat{\vartheta}_i^{t-1}$
- 15 Output final set of bundle–value pairs $\hat{\vartheta}^T$, where $T = t$

The estimated social welfare function in Line 4 of Algorithm 1, $\tilde{V}^t = \mathcal{A}(\hat{\vartheta}^{t-1}) : \mathcal{X}^n \rightarrow \mathbb{R}_+$, will be decomposed into

$$\tilde{V}^t(\cdot) = \sum_{i \in N} \tilde{v}_i^t(\cdot),$$

where $\tilde{v}_i^t(\cdot)$ estimates the true valuation function $v_i(\cdot)$ of bidder i and is trained on the data set $\hat{\vartheta}_i^{t-1}$, i.e., the queried values up to round $t - 1$.

Instead of using an SVR as it was successfully done in Brero et al. (2018), we model \tilde{v}_i^t using a DNN, $\mathcal{NN}_i : \{0, 1\}^m \rightarrow \mathbb{R}_+$, with rectified linear units (ReLU) $\varphi : \mathbb{R} \rightarrow \mathbb{R}_+$, $\varphi(s) := \max(0, s)$, as activation functions for each node. These act on vectors component wise, i.e., for $s \in \mathbb{R}^k$ let $\varphi(s) := (\varphi(s_1), \dots, \varphi(s_k))$.

Therefore, \tilde{V}^t is modeled as a sum of fully connected feed forward neural networks: $\tilde{V}^t(\cdot) := \sum_{i \in N} \mathcal{NN}_i(\cdot)$. The exact parameterization of each \mathcal{NN}_i will be discussed in the next section.

Our first objective then is to reformulate and to efficiently solve in each iteration the optimization problem described in line (5) of Algorithm 1, which we call in the following the *optimization step*.

3 MILP Formulation for the Maximization of DNNs

In this section, we reformulate the *optimization step* of the preference elicitation algorithm as a MILP, given trained DNNs. We focus on Line (5) of Algorithm 1 for a fixed iteration step t . For the sake of readability, we no longer highlight the dependency on t of all objects considered in the following.

First we define the parameters of the DNNs in our setting. Each \mathcal{NN}_i consists of $K - 1$ hidden layers for $K \in \mathbb{N}$, which contain d_k hidden units each, where $k \in \{1, \dots, K - 1\}$. Let $d_0 := m$ be the dimension of the input bundle/input layer x^i and $d_K := 1$ be the dimension of the output/final layer. Thus, a single DNN consists in total of $K + 1$ layers (including the input and the output

layer). Furthermore, let φ denote the ReLU activation function defined in the previous section. The affine components of each layer are parameterized by a matrix $W^{i,k} \in \mathbb{R}^{d_{k+1} \times d_k}$ and a bias $b^{i,k} \in \mathbb{R}^{d_{k+1}}$, $k \in \{0, \dots, K-1\}$. These quantities are estimated in line (4) of Algorithm 1 and can be considered as constants in the following analysis.

To sum up, given affine parameters $W := \{W^{i,k}\}_{\{i,k\} \in N \times \{0, \dots, K-1\}}$ and $b := \{b^{i,k}\}_{\{i,k\} \in N \times \{0, \dots, K-1\}}$ each DNN $\mathcal{NN}_i(W, b)$ represents the following function:

$$\begin{aligned} \{0, 1\}^m &\rightarrow \mathbb{R}_+ \\ x^i &\mapsto \varphi(W^{i,K-1} \varphi(W^{i,K-2} \varphi(\dots \varphi(W^{i,1} \varphi(W^{i,0} x^i + b^{i,0}) + b^{i,1}) \dots) + b^{i,K-2}) + b^{i,K-1}) \end{aligned} \quad (1)$$

A schematic representation of a single deep neural network \mathcal{NN}_i is given in Figure 1.

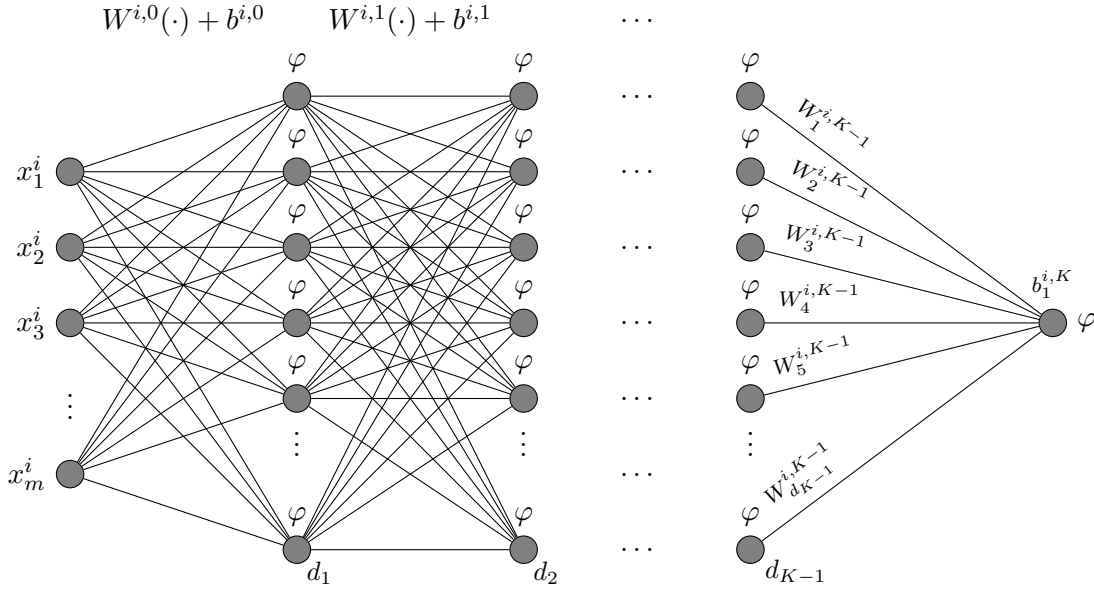


Figure 1: Schematic representation of a single deep neural network $\mathcal{NN}_i : \mathcal{X} \rightarrow \mathbb{R}_+$ with $K-1$ hidden layers; The total number m of items is equal to the dimension of the input; for each node the ReLU activation function φ is used; dimensions of each layer are denoted at the bottom by d_i .

Given the fitted parameters $\widehat{W} := \{\widehat{W}^{i,k}\}_{\{i,k\} \in N \times \{0, \dots, K-1\}}$ and $\widehat{b} := \{\widehat{b}^{i,k}\}_{\{i,k\} \in N \times \{0, \dots, K-1\}}$ obtained in line (4) of Algorithm 1, the goal is to solve the following optimization problem:

Problem 2 (OPTIMIZATION STEP). Given fitted parameters \widehat{W} and \widehat{b} and the corresponding DNNs $\mathcal{NN}_i(\widehat{W}, \widehat{b})$, $i \in N$, the optimization problem of the preference elicitation algorithm, Algorithm 1, is given by

$$\begin{aligned} & \max_{x \in \mathcal{X}^n} \left\{ \sum_{i \in N} \mathcal{NN}_i(\widehat{W}, \widehat{b})(x^i) \right\} \\ \text{s.t.} & \\ & \sum_{i \in N} x_j^i \leq 1, \quad \forall j \in M, \\ & x_j^i \in \{0, 1\}, \quad \forall j \in M, \forall i \in N. \end{aligned} \tag{P1}$$

By introducing for each layer $k \in \{0, \dots, K-1\}$, d_k binary decision variables $y^{i,k} \in \{0, 1\}^{d_k}$, that represent which node in the corresponding layer is active, as well as $2 \cdot d_k$ continuous variables $z^{i,k}, s^{i,k} \in \mathbb{R}^{d_k}$, where $z^{i,k}$ corresponds to the positive part of the output value of each layer and $s^{i,k}$ is used as a slack variable representing the negative part of the output value, we are able to reformulate problem (P1) into a MILP.

The basic idea is to encode each activation function, i.e, each maximum function appearing in the definition of \mathcal{NN}_i , $i \in N$, as multiple linear constraints.

Let $o^{i,k} \in \mathbb{R}_+^{d_k}$, $k \in \{1, \dots, K\}$ be the output (node values) of the k^{th} layer. Then we are able to recursively calculate the output of the next layer given the previous one by

$$o^{i,k} = \varphi(\widehat{W}^{i,k-1} o^{i,k-1} + \widehat{b}^{i,k-1}) = \max(0, \widehat{W}^{i,k-1} o^{i,k-1} + \widehat{b}^{i,k-1}). \tag{2}$$

In the next lemma we show how to encode $o^{i,k}$ using linear constraints only.

Lemma 3.1. Let $z^{i,k}, s^{i,k} \in \mathbb{R}^{d_k}$, $y^{i,k} \in \{0, 1\}^{d_k}$, $k \in \{1, \dots, K\}$, and L be a large positive constant. Furthermore, consider for a fixed value of $\widehat{W}^{i,k-1} o^{i,k-1} + \widehat{b}^{i,k-1}$ the polytope defined by the following linear inequalities:

$$z^{i,k} - s^{i,k} = \widehat{W}^{i,k-1} o^{i,k-1} + \widehat{b}^{i,k-1} \tag{3}$$

$$0 \leq z^{i,k} \leq y^{i,k} \cdot L \tag{4}$$

$$0 \leq s^{i,k} \leq (1 - y^{i,k}) \cdot L. \tag{5}$$

Then this polytope is not empty and every element $((z^{i,k})^*, (s^{i,k})^*, (y^{i,k})^*)$ of this polytope satisfies that

$$(z^{i,k})^* = o^{i,k},$$

where $o^{i,k}$ was defined in (2).

Proof. Let $a := \widehat{W}^{i,k-1} o^{i,k-1} + \widehat{b}^{i,k-1}$. From constraints (4) and (5) it follows for each $j \in \{1, \dots, d_k\}$ that if $(z^{i,k})_j > 0$ then $(s^{i,k})_j = 0$ and vice versa. We have to distinguish the following three cases for each component of a :

1. $a_j < 0 \implies (y^{i,k})_j^* = 0, (z^{i,k})_j^* = 0 = \varphi(a_j)$ and $(s^{i,k})_j^* = -a_j$.
2. $a_j > 0 \implies (y^{i,k})_j^* = 1, (s^{i,k})_j^* = 0$ and $(z^{i,k})_j^* = a_j = \varphi(a_j)$.
3. $a_j = 0 \implies \left((z^{i,k})_j^*, (s^{i,k})_j^*, (y^{i,k})_j^* \right) = (0, 0, 1)$ or $\left((z^{i,k})_j^*, (s^{i,k})_j^*, (y^{i,k})_j^* \right) = (0, 0, 0)$, and in both cases it holds that $(z^{i,k})_j^* = 0 = \varphi(a_j)$.

Combining these cases yields that $(z^{i,k})^* = o^{i,k}$ as claimed. \square

Before we discuss the general reformulation into the MILP, we highlight the application of Lemma 3.1 via a simple example considering only one agent ($n = 1$), m items ($d_0 = m$) and one hidden layer ($K = 2$).

Example 1. Given $\widehat{W}^{1,0} \in \mathbb{R}^{d_1 \times m}$, $\widehat{W}^{1,1} \in \mathbb{R}^{1 \times d_1}$ and $\hat{b}^{1,0} \in \mathbb{R}^{d_1}$, $\hat{b}^{1,1} \in \mathbb{R}$, consider the maximization problem defined in (P2)³:

$$\begin{aligned} \max_{x^1 \in \mathcal{X}^1} \mathcal{N}_1(\widehat{W}, \hat{b})(x^1) &= \max_{x^1 \in \mathcal{X}^1} \left\{ \max \left(0, \widehat{W}^{1,1} \max \left(0, \widehat{W}^{1,0} x^1 + \hat{b}^{1,0} \right) + \hat{b}^{1,1} \right) \right\} \\ \text{s.t.} & \\ x_j^1 &\in \{0, 1\}, \quad \forall j \in M. \end{aligned}$$

Let $L \in \mathbb{R}_+$ be a large constant. In a first step, we replace the inner maximum by using $y^{1,1} \in \{0, 1\}^{d_1}$ and $z^{1,1}, s^{1,1} \in \mathbb{R}^{d_1}$ and arrive at the equivalent optimization problem

$$\begin{aligned} \max_{x^1 \in \mathcal{X}^1, z^{1,1}, s^{1,1}, y^{1,1}} &\left\{ \max \left(0, \widehat{W}^{1,1} z^{1,1} + \hat{b}^{1,1} \right) \right\} \\ \text{s.t.} & \\ z^{1,1} - s^{1,1} &= \widehat{W}^{1,0} x^1 + \hat{b}^{1,0}, \\ 0 &\leq z^{1,1} \leq y^{1,1} \cdot L, \\ 0 &\leq s^{1,1} \leq (1 - y^{1,1}) \cdot L, \\ x_j^1 &\in \{0, 1\}, \quad \forall j \in M. \end{aligned}$$

Applying the same trick again to the new objective function using additional variables $y^{1,2} \in \{0, 1\}$

³The constraint $\sum_{i \in N} x_j^i \leq 1, \forall j \in M$ of problem (P1) is redundant in this case, since we only consider one agent.

and $z^{1,2}, s^{1,2} \in \mathbb{R}$ yields the final MILP formulation

$$\begin{aligned}
& \max_{x^1 \in \mathcal{X}^1, z^{1,k}, y^{1,k}, s^{1,k}} \{z^{1,2}\} \\
& \text{s.t.} \\
& z^{1,1} - s^{1,1} = \widehat{W}^{1,0} x^1 + \widehat{b}^{1,0}, \\
& 0 \leq z^{1,1} \leq y^{1,1} \cdot L, \\
& 0 \leq s^{1,1} \leq (1 - y^{1,1}) \cdot L, \\
& \\
& z^{1,2} - s^{1,2} = \widehat{W}^{1,1} z^{1,1} + \widehat{b}^{1,1}, \\
& 0 \leq z^{1,2} \leq y^{1,2} \cdot L, \\
& 0 \leq s^{1,2} \leq (1 - y^{1,2}) \cdot L, \\
& \\
& x_j^1 \in \{0, 1\}, \quad \forall j \in M.
\end{aligned}$$

Gathering all results together, we can finally state the following proposition, which presents the reformulation of the optimization problem (P1) into a MILP when using DNNs with ReLu activation functions as the ML-algorithm in the preference elicitation algorithm.

Proposition 3.1. (MILP FORMULATION OF THE OPTIMIZATION STEP)

Let $\mathcal{NN}_i(\widehat{W}, \widehat{b})$ for $i \in N$ be defined as in (1) given fitted parameters \widehat{W} and \widehat{b} . Furthermore, let $x \in \mathcal{X}^n$ and $y^{i,k} \in \{0, 1\}^{d_k}$ and $z^{i,k}, s^{i,k} \in \mathbb{R}^{d_k}, \forall k \in \{1, \dots, K\}$ and L be a large positive constant. Then the following MILP is equivalent to the optimization problem of the preference elicitation algorithm defined earlier in (P1).

$$\begin{aligned}
& \max_{x \in \mathcal{X}^n, z^{i,k}, s^{i,k}, y^{i,k}} \left\{ \sum_{i \in N} z^{i,K} \right\} \\
& \text{s.t.} \tag{P2} \\
& \left. \begin{aligned}
& z^{i,0} = x^i \\
& z^{i,k} - s^{i,k} = \widehat{W}^{i,k-1} z^{i,k-1} + \widehat{b}^{i,k-1} \\
& 0 \leq z^{i,k} \leq y^{i,k} \cdot L \\
& 0 \leq s^{i,k} \leq (1 - y^{i,k}) \cdot L \\
& y^{i,k} \in \{0, 1\}^{d_k}
\end{aligned} \right\} k = 1, \dots, K, i = 1, \dots, n, \\
& \\
& x_j^i \in \{0, 1\}, \quad j = 1, \dots, d_0, i = 1, \dots, n \\
& \sum_{i \in N} x_j^i \leq 1, \quad j = 1, \dots, d_0.
\end{aligned}$$

Using this reformulation we are able to solve the *optimization step* in the preference elicitation algorithm using standard optimization packages like CPLEX.

Remark 1. *The number of decision variables in the MILP defined in (P2) is given by*

$$\underbrace{n}_{\#bidders} \cdot \left(\underbrace{m}_{\#items \text{ or input}} + \underbrace{3}_{y^{k,i}, s^{k,i} \text{ and } z^{k,i}} \cdot \left(\sum_{k=1}^{\overbrace{K-1}^{\#hidden \text{ layers}}} \underbrace{d_k}_{\#hidden \text{ units}} + \underbrace{1}_{output} \right) \right).$$

4 Experimental Design

In this section we present results on (i) the estimation performance of DNNs (4.2), (ii) the resulting efficiency of the preference elicitation algorithm (4.3) and (iii) the efficiency and revenue obtained from the entire deep learning-powered ICA mechanism, which will be presented in detail in Section 4.4.

4.1 Local Synergy Value Model

For the experimental evaluation of the estimation accuracy of DNNs, we use the spectrum auction test suite (SATS) (Weiss et al., 2017). Specifically, we compare the estimation performance of the previously defined DNNs to SVRs in the Local Synergy Value Model (LSVM), which was introduced in Scheffel et al. (2012). This choice was made, since SVRs performed worst in LSVM, thus providing the most room for improvement – with respect to total efficiency in the whole auction mechanism – compared to all other value models available in SATS.

LSVM consists of 18 items. These are arranged on a rectangle of size 3×6 . Complementarities of the items arise from spatial proximity. This model contains two different types of bidders: one *national bidder*, who is interested in all items, and five *regional bidders*. Each *regional bidder* is interested in a randomly drawn most preferred item, all horizontal and vertical adjacent items, and the horizontal and vertical items adjacent to those. Using SATS, we generate a data set for the LSVM model, of given bundle–value pairs $\{(x^i)^{(k)}, v_i((x^i)^{(k)})\}_{k \in K_i \subset \mathbb{N}}$ for all bidders $i \in N$. Details of how the value function of each bidder is defined, can be found in Scheffel et al. (2012), Section 3.2.2. Figure 2 and Figure 3 show all bundle–value pairs sampled from a single LSVM instance.

In Figure 2 each bidder’s valuation of all bundles $v_i((x^i)^{(k)})$, $k \in \{1, \dots, 2^{18}\}$ is plotted against the number of items contained in the bundle, i.e., $|\{j \in M : [(x^i)^{(k)}]_j = 1\}|$.

Valueplots LSMV: Regional bidders = {1,2,3,4,5}, National bidder = {0}

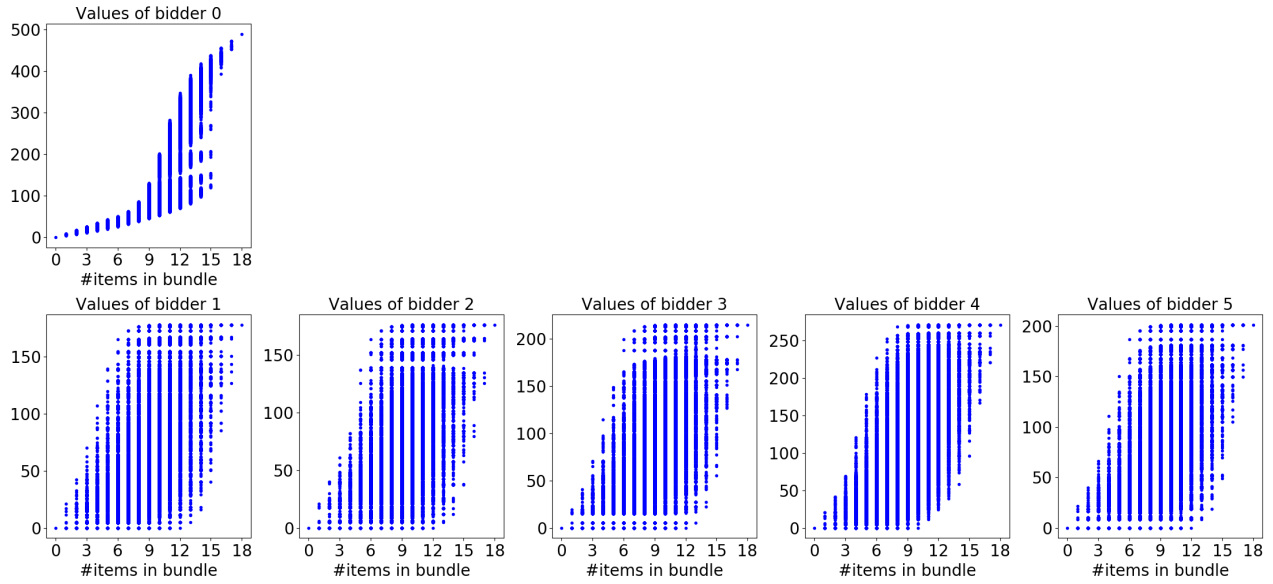


Figure 2: Bidders' true valuations of all 2^{18} bundles drawn from a single LSMV instance

Figure 3 presents a boxplot of the bidders' valuations.

Boxplots LSMV: Regional bidders = {1,2,3,4,5}, National bidder = {0}

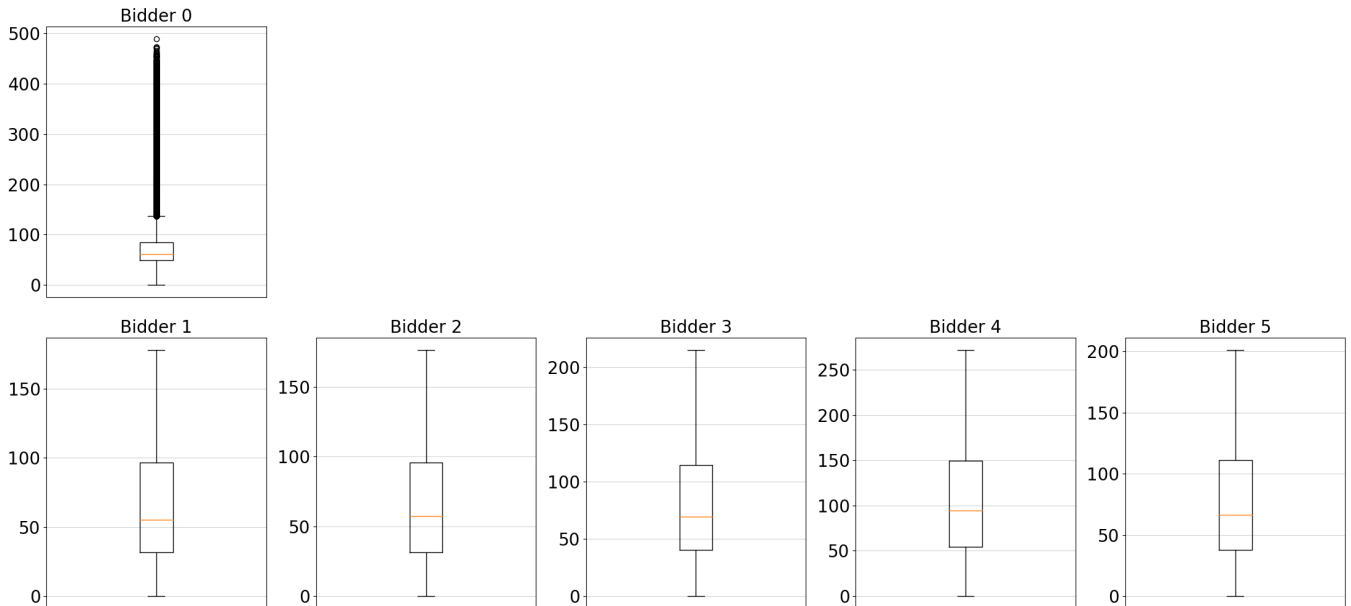


Figure 3: Bidders' true valuations of all 2^{18} bundles drawn from a single LSMV instance.

4.2 Experimental Results: Estimation Accuracy

In this section, we compare the learning capabilities of DNNs to SVRs in the previously introduced LSVM. The experimental design for DNNs is described in Algorithm 2. The same design was used for SVRs.

Algorithm 2: MEASURING ESTIMATION ACCURACY OF DNNs IN THE LSVM

Data: Bundle–value pairs drawn from different instances of the LSVM

Result: Mean absolute error (MAE)⁴ for each bidder type i in $\{\text{national}, \text{regional}\}$ averaged across LSVM instances on a training and a validation set: $\text{MAE}_{\text{train}}(i)$, $\text{MAE}_{\text{valid}}(i)$

```

1 Draw  $L$  instances of the LSVM randomly  $\{\mathcal{L}_1, \dots, \mathcal{L}_L\}$ ;
2 for each  $\mathcal{L}_l$  do
3   for each bidder type  $i$  in  $\{\text{national}, \text{regional}\}$  do
4     Sample  $T + V$  bundle–value pairs  $\{(x^i)^{(k)}, v_i((x^i)^{(k)}))\}_{k \in \{1, \dots, T+V\}}$  from  $\mathcal{L}_l$  and split them
       into a training set  $\mathcal{T}_l^i$  of size  $T$  and a validation  $\mathcal{V}_l^i$  set of size  $V$ ;
5     Fit a DNN  $\mathcal{NN}_i(\widehat{W}, \widehat{b})$  on  $\mathcal{T}_l^i$  using the MAE5 as the corresponding loss function;
6     Calculate and save the corresponding MAE on the training and validation set and obtain
        $\text{MAE}_{\text{train}}(l, i)$  and  $\text{MAE}_{\text{valid}}(l, i)$ ;
7   end
8 end
9 Average the errors and obtain  $\forall i : \text{MAE}_{\text{train/valid}}(i) := \frac{1}{L} \sum_{l=1}^L \text{MAE}_{\text{train/valid}}(l, i)$ 

```

Using Algorithm 2, we now measure the generalization performance of DNNs and SVRs. The following results were obtained by setting $L := 200$, $T := 100$ and $V := 1000$. This unusual split was chosen to capture a real-world CA, where the number of initial bids is usually rather small compared to the number of possible bids.

For the architecture of a single DNN, we choose a two-hidden-layer feed-forward-fully-connected neural network $\mathcal{NN}_i(W, b)$ for each bidder i , in which each hidden layer consisted of maximal 16 hidden units. Investigating larger architectures, their influence on the estimation accuracy and the resulting scalability of the MILP in (P2) is postponed to future work. The previously defined parameters were set to:

1. $\mathbf{n} := 6$ (number of bidders in the LSVM)
2. $\mathbf{m} := \mathbf{d}_0 = 18$ (number of items in the LSVM)
3. $\mathbf{K} - \mathbf{1} := 2$ (number of hidden layers)

Besides that, we conducted a minimal hyper-parameter optimization for each individual DNN via a heuristic grid search over the following parameters:

1. Dimension of the hidden layers $\mathbf{d}_k, \forall k \in \{1, 2\}$.
2. A single L2-regularization parameter $\lambda \geq 0$ applied to W and b .
3. Learning Rate $\eta > 0$ of the ADAM algorithm (Kingma and Ba, 2014).
4. Dropout rate during training denoted by *dropout*.

The remaining parameters for the fitting process were selected equally across all neural networks as follows:

1. Number of epochs $N_E := 512$.
2. Batch size $B_S := 32$.

All experiments were conducted in Python 3.6 using the open source machine learning library *Tensorflow* with the high level *Keras functional API*.

In Table 1, estimation results of different kernelized SVRs and DNNs are presented. We sampled 200 instances of the LSVM with default configuration, i.e, 5 *regional bidders* and 1 *national bidder*. For each bidder-type, we present the MAE averaged over instances on a randomly sampled training and validation set for the configuration of hyper-parameters that achieved the minimal MAE on the validation set.⁶ Standard errors are shown in parentheses.

Model	kernel: $k(x, y)$	bidder type	C	ϵ	γ	degree q	r	MAE _{Train}	MAE _{Valid}
SVR	$x^T y$	National	1	0.01	None	None	None	54.93 (0.488)	70.24 (0.586)
		Regional	1	0.01	None	None	None	17.67 (0.269)	23.83 (0.363)
	$x^T y + \gamma(x^T y)^q$	National	1	0.01	0.01	2	None	9.85 (0.133)	40.62 (0.240)
		Regional	1	0.01	0.001	2	None	7.43 (0.121)	13.89 (0.200)
	$(\gamma \cdot x^T y + r)^q$	National	1	0.01	auto ⁷	4	0	13.44 (0.164)	30.02 (0.175)
		Regional	1	0.001	auto	6	1	0.42 (0.002)	13.10 (0.185)
		National	1	0.01	auto	2	1	17.81 (0.199)	38.71 (0.225)
		Regional	1	0.01	auto	2	1	4.85 (0.061)	13.35 (0.191)
	$e^{(x^T y) \cdot \gamma}$	National	1	0.01	0.1	None	None	6.80 (0.094)	36.05 (0.213)
		Regional	1	0.01	0.1	None	None	3.79 (0.021)	13.08 (0.187)
	$e^{-(\ x-y\ _2^2 \cdot \gamma)}$	National	1	0.01	scale ⁸	None	None	5.95 (0.077)	37.19 (0.210)
		Regional	10	0.001	scale	None	None	0.04 (0.0002)	12.90 (0.178)

Model	#hidden layers	bidder type	λ	η	d_k	dropout	-	MAE _{Train}	MAE _{Valid}
DNN	2	National	0.00001	0.01	10	0.05	-	12.72 (0.257)	29.88 (0.262)
	2	Regional	0.00001	0.01	16	0.05	-	6.236613 (0.158)	12.82 (0.193)

Table 1: Estimation error measured in terms of MAE averaged over 200 Instances and bidder types.

It is noteworthy that the estimation error across models of the national bidder’s valuation function is significantly larger than for the other regional bidders. One possible explanation is that the distribution of bundle valuations of national bidders has several large outliers (as can be seen in Figure 3 top-left plot) for a national bidder in a generated LSVM instance.

⁴Similarly as in Brero et al. (2018), we used MAE to measure estimation accuracy.

⁵This first choice was made in accordance to the ϵ -sensitive loss, that defines SVRs. Investigation of other loss functions is postponed to future work.

⁶Except for the third kernel, we additionally reported the best configuration for degree 2 in order to have a comparison to the second kernel.

⁷‘auto’ is a predefined kernel coefficient in SCIKIT-LEARN SVR and is equal to $\frac{1}{\#features}$

⁸‘scale’ is a predefined kernel coefficient in SCIKIT-LEARN SVR and is equal to $\frac{1}{\#features \cdot X.var()}$

The larger estimation error of national bidders compared to regional bidders can also be observed when comparing Figure 4 (national-bidder-type) to Figure 5 (regional-bidder-type). In each of these figures, we present two plots given a DNN, which was trained ($N_E := 500, B_S = 50$) on 100 and validated on 1000 randomly sampled bundle-value pairs generated from a single LSVM instance. The left plot shows how the training and validation error evolves in the number of epochs (\propto number of gradient descent steps taken) during training. The right plot presents the prediction accuracy of the trained DNN on the training set as well as on the validation set. Ideally, all the points would lie on the black identity line.

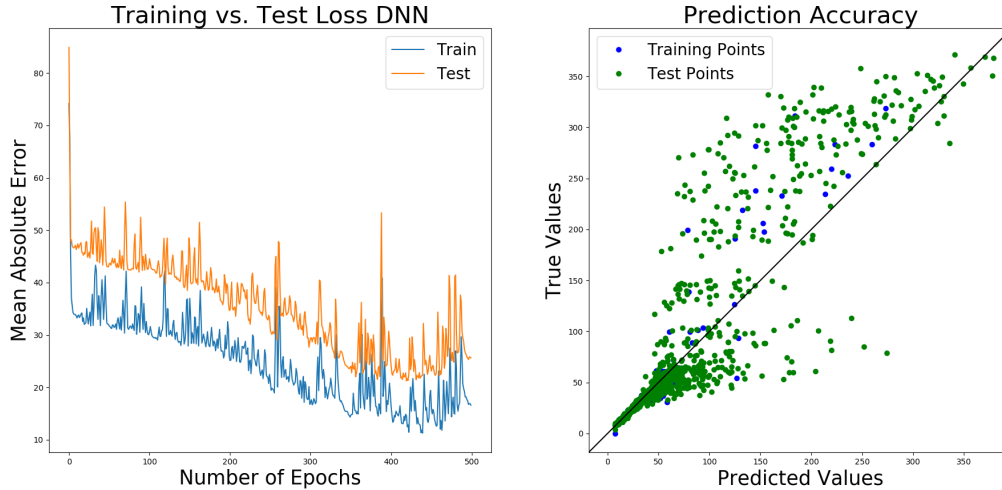


Figure 4: **National Bidder**; Left: evolution of the training and validation loss in the number of epochs. Right: True valuation vs. predicted valuations from the fitted DNN.

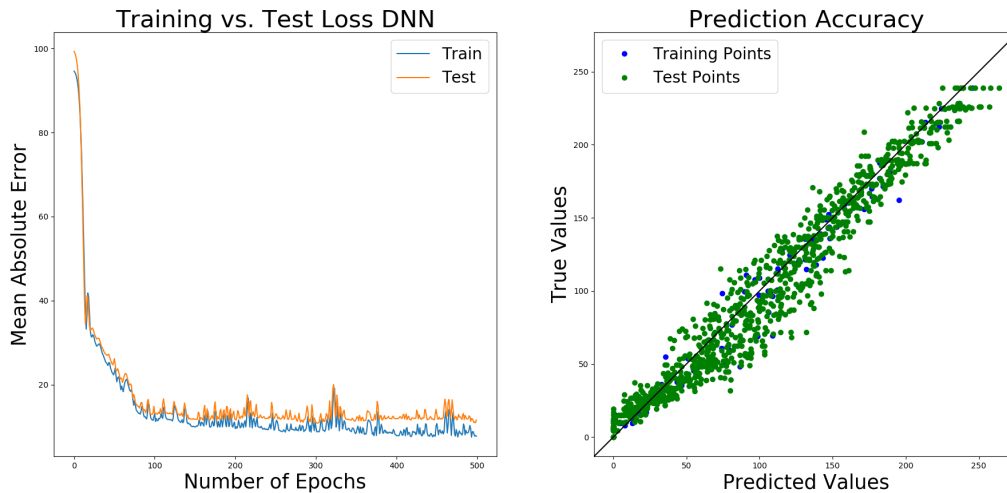


Figure 5: **Regional Bidder**; Left: evolution of the training and validation loss in the number of epochs. Right: True valuation vs. predicted valuations from the fitted DNN.

From Table 1 we can infer that even with a minimal hyper-parameter optimization and a rather

small and a priori defined architecture, DNNs can better capture the valuation functions than kernelized SVRs. Specifically, their performance is better than the ones obtained when using a gaussian, exponential or high-degree polynomial kernel in the definition of the SVRs. Additionally, as mentioned in the introduction, the *optimization step* for these kernels was computationally expensive and for large auctions even intractable. For a single MILP of the form (P2) a one-hour cap on the computing time was set in Brero et al. (2018). When using more expressive kernels this cap was reached in almost all cases in the LSVM.

In contrast, we were able to solve a single MILP for LSVM of the form (P2), for an estimated social welfare function $\tilde{V}^t(\cdot) = \sum_{i \in N} \tilde{v}_i^t(\cdot) = \mathcal{NN}_i(\widehat{W}, \widehat{b})(\cdot)$ in roughly 10 seconds using the Python API of *CPLEX 12.8* on a *Intel Core i7-8650U laptop with 16GB of RAM*. Given our selected DNN architectures, the number of variables and constraints of the resulting MILP (P2) can be calculated using Remark 1 and is presented in Table 2.

variables		constraints
# binary variables	# continuous variables	# linear constraints
306	396	612

Table 2: Number of variables and constraints in the MILP.

These results strongly suggest that DNNs provide promising results for having, on the one hand, better estimation accuracy than linear and quadratic kernels and on the other hand for resulting in a faster solvable *optimization step*. Investigating the scalability of the resulting optimization step for larger neural network architectures is postponed to future work.

4.3 Experimental Results: Efficiency of the Preference Elicitation Algorithm

In this section, we present results on the efficiency of the preference elicitation algorithm, Algorithm 1, when using DNNs. As mentioned earlier, real world CAs usually impose a cap κ on the number of bundles for which bidders can report a value (see Problem 1). Analogously to Brero et al. (2018), we set the total number of queries asked during Algorithm 1 to 50, i.e., $\kappa := 50$. The number of initially reported bundle–value pairs per bidder in Algorithm 1, denoted by $c_0 := |\hat{v}_i^0|, \forall i \in N$, was set equally across bidders to 40. Thus, resulting in at maximum $\kappa - c_0 = 10$ remaining queries, which could be elicited during the algorithm.

The efficiency of the preference elicitation method is measured by comparing the true social welfare of the optimal allocation $x_{\hat{v}}^*$ given the output of Algorithm 1, i.e, the elicited bundle–value pairs \hat{v} to the true optimal allocation x^* , i.e,

$$\frac{V(x_{\hat{v}}^*)}{V(x^*)},$$

where $x_{\hat{v}}^* \in \arg \max_{x \in \mathcal{F}} \widehat{V}(x, \hat{v})$ and $x^* \in \arg \max_{x \in \mathcal{F}} V(x)$. Note that using SATS we have access to the quantities $x^*, V(x^*)$ as well as $V(x_{\hat{v}}^*)$, which would usually not be the case in a real-world auction setting.

For the architectures of the DNNs, we conducted the same experiment as described in Section 4.2 using a training set of size 40 and finally selected the architectures and hyper-parameters according to their performance on a validation set of size 1000. The selected parameters are presented in Table 3. Results of the simulations are shown in Figure 6.

Model	#hidden layers	bidder type	λ	η	d_k	dropout
DNN	2	National	0.00001	0.05	8	0.1
	2	Regional	0.0001	0.01	16	0.1

Table 3: Selected DNN parameters for the preference elicitation algorithm.

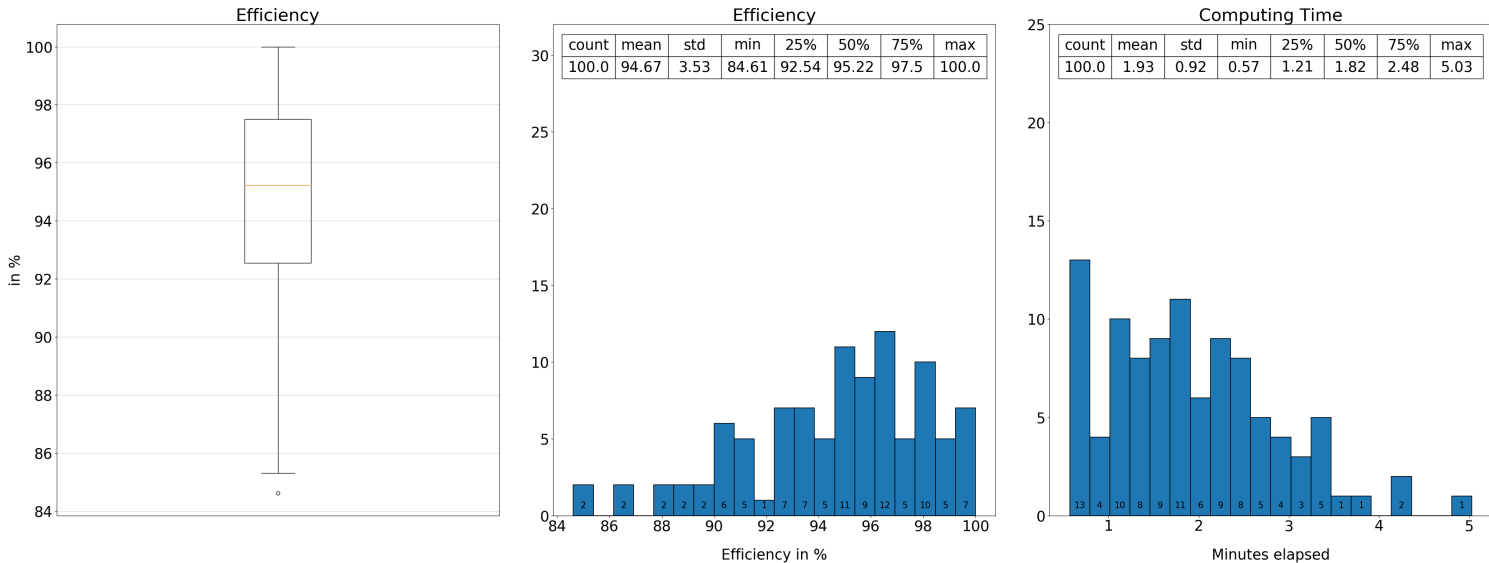


Figure 6: Efficiency and computing time of the preference elicitation method for 100 Instances.

As can be observed from Figure 6, we were able to achieve an average efficiency of **94.67%**(0.35%), which is an increase of about 1.2 percentage points compared to the average efficiency of the preference elicitation algorithm based on SVRs of **93.5%**(0.4%)⁹, that was reported in [Brero et al. \(2018\)](#). These results show that using DNNs for preference elicitation can lead to more efficient allocations. Investigating the resulting efficiency of the preference elicitation algorithm for larger DNN architectures is postponed to future work.

⁹Standard errors are shown in parentheses. The 95%-normal-confidence interval in [Brero et al. \(2018\)](#) is given by [92.7%, 94.3%]

4.4 Experimental Results: Pseudo-VCG Mechanism (PVM)

Finally, we evaluate DNNs on the entire PVM auction mechanism as in Brero et al. (2018). PVM calls Algorithm 1 $n + 1$ times; Once including all bidders (main economy) and n times by excluding in each run a single different bidder (marginal economies). This procedure, which is inspired by the VCG mechanism, was conducted to obtain payments such that the auction is *incentive aligned*. The PVM mechanism, as defined in Brero et al. (2018), is presented in Algorithm 3 (with minor changes):

Algorithm 3: PSEUDO-VCG MECHANISM (following Brero et al. (2018))

- 1 Run Algorithm 1 $n + 1$ times and obtain for each run an elicited set of reported bundle-value pairs:

$$\hat{v}^{(-\emptyset)}, \hat{v}^{(-1)}, \dots, \hat{v}^{(-n)}.^a$$

- 2 Calculate

$$\hat{v}^{pvm} := \hat{v}^{(-\emptyset)} \cup \bigcup_{i \in N} \hat{v}^{(-i)}.$$

- 3 Determine for each set of elicited bids in the marginal economies the optimal allocations:

$$x^{(-1)}, \dots, x^{(-n)}, \quad \text{where } x^{(-i)} \in \arg \max_{x \in \mathcal{F}} \widehat{V}(x, \hat{v}^{(-i)}).$$

- 4 Calculate the final allocation of the PVM mechanism as:

$$x^{pvm} \in \arg \max_{x \in \mathcal{F}} \widehat{V}(x, \hat{v}^{pvm}).$$

- 5 Calculate the payments $p^{pvm} := (p_1^{pvm}, \dots, p_n^{pvm})$ by charging each bidder $i \in N$ according to:

$$p_i^{pvm} := \sum_{j \neq i: ([x^{(-i)}]_j, \hat{v}_j([x^{(-i)}]_j)) \in \hat{v}_j^{(-i)}} \hat{v}_j([x^{(-i)}]_j) - \sum_{j \neq i: ([x^{pvm}]_j, \hat{v}_j([x^{pvm}]_j)) \in \hat{v}_j^{pvm}} \hat{v}_j([x^{pvm}]_j).$$

- 6 Output final allocation and corresponding payments: $\{x^{pvm}, p^{pvm}\}$.
-

^a $\hat{v}^{(-i)}$ denotes the output of Algorithm 1 by excluding bidder i from the set of bidders.

Analogously to Brero et al. (2018), for the evaluation of the PVM mechanism we set $\kappa := 100$.¹⁰ Furthermore we set $c_0 := 75$. The following experiments were conducted by using two-hidden-layer DNNs, which have been proven to outperform SVRs with respect to estimation accuracy and obtained efficiency in the preference elicitation algorithm. The remaining parameters of the DNNs were again selected according to the estimation performance on a validation set and are given in Table 4.

Model	#hidden layers	bidder type	λ	η	d_k	dropout
DNN	2	National	0.00001	0.01	10	0.05
	2	Regional	0.0001	0.01	16	0.1

Table 4: Selected DNN parameters for the PVM mechanism.

¹⁰Note that the query cap κ is now defined for the full PVM mechanism across all $n + 1$ elicitation runs and not for each individual elicitation run. Thus, we ensure that each bidder is at most queried κ times during the entire auction.

Results are shown in Figure 7.

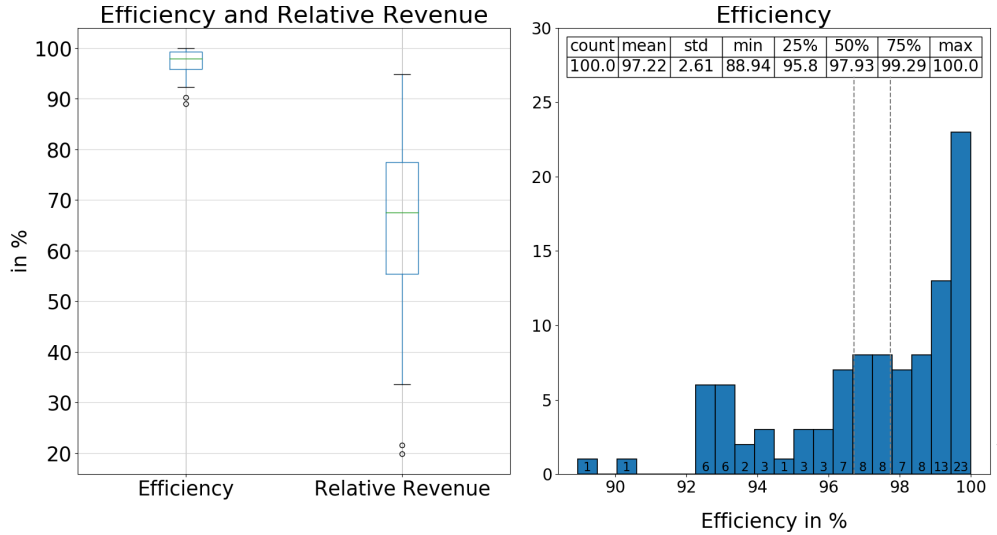


Figure 7: Efficiency and relative revenue of the PVM mechanism evaluated on 100 Instances of the LSVM. A 95%-basic-bootstrapped-confidence interval is shown in gray lines in the histogram plot. Revenue is defined as $\sum_{i \in N} p_i^{pvm}$. Relative revenue is calculated according to $\frac{\sum_{i \in N} p_i^{pvm}}{V(x^*)}$.

Figure 7 shows that, by using DNNs, we are able to obtain an average efficiency resulting from the PVM mechanism of **97.22%**(0.26%). Compared to the reported number of **96.5%**(0.4%) in Brero et al. (2018) , this is an increase of about 0.7 percentage points. Note that even small differences in efficiency can have a very large monetary impact, considering that one of the most popular applications of CAs are multi-billion-dollar spectrum auctions. Overall, these results show that using DNNs in an ICA for preference elicitation can lead to a significant increase in efficiency. Investigating the performance of larger and more tuned networks is postponed to future work. These could potentially lead to even higher efficiency.

5 Conclusion

In this paper, we have investigated the design of deep learning-powered iterative combinatorial auctions. Our experimental results have shown that DNNs can improve preference elicitation compared to using SVRs with respect to both computational time of the *optimization step* and estimation accuracy. Furthermore, by using small-sized two-hidden-layer DNNs, we were able to obtain more efficient allocations in both the preference elicitation algorithm and the entire auction mechanism (PVM).

Investigating if larger and more fine-tuned DNN architectures can further increase efficiency is an important task for future research. It will be crucial to investigate the trade-off between scalability of the *optimization step* and the *economic efficiency* of the auction mechanism with increasing model complexity (number of hidden layers and units).

References

Brero, G., Lubin, B., and Sven, S. (2018). Combinatorial auctions via machine learning-based preference elicitation. In *Proceedings of the 27th International Joint Conference on Artificial In-*

telligence and the 23rd European Conference on Artificial Intelligence (IJCAI-ECAI), Stockholm, Sweden.

Fischetti, M. and Jo, J. (2017). Deep neural networks as 0-1 mixed integer linear programs: A feasibility study. CoRR, abs/1712.06174.

Kingma, D. P. and Ba, J. (2014). Adam: A method for stochastic optimization. *arXiv preprint arXiv:1412.6980*.

Nisan, N. and Segal, I. (2006). The communication requirements of efficient allocations and supporting prices. *Journal of Economic Theory*, 129(1):192–224.

Scheffel, T., Ziegler, G., and Bichler, M. (2012). On the impact of package selection in combinatorial auctions: an experimental study in the context of spectrum auction design. *Experimental Economics*, 15(4):667–692.

Smola, A. J. and Schölkopf, B. (2004). A tutorial on support vector regression. *Statistics and computing*, 14(3):199–222.

Weiss, M., Lubin, B., and Seuken, S. (2017). Sats: A universal spectrum auction test suite. In *Proceedings of the 16th Conference on Autonomous Agents and MultiAgent Systems*, pages 51–59. International Foundation for Autonomous Agents and Multiagent Systems.